Detection of a Stable Intermediate in the Thermal Unfolding of a Cysteine-Free Form of Dihydrofolate Reductase from *Escherichia coli*†

J. Luo, M. Iwakura,‡ and C. R. Matthews*

Department of Chemistry and Center for Biomolecular Structure and Function, The Pennsylvania State University, University Park, Pennsylvania 16802

Received April 24, 1995; Revised Manuscript Received June 13, 1995®

ABSTRACT: The reversible temperature-induced unfolding of a cysteine-free mutant (C85S/C152E, des-Cys) of dihydrofolate reductase from *Escherichia coli* has been studied by absorbance and by both far- and near-ultraviolet circular dichroism spectroscopies. The non-coincidence of all three transition curves demonstrated the existence of a highly populated partially-folded form near 39 °C at pH 7.8. This intermediate retains substantial secondary structure and partially excludes one or more of the five tryptophans from solvent; however, the intermediate has lost specific tertiary packing around its aromatic residues. Increases in enthalpy, entropy, and heat capacity are observed for both the native/intermediate and intermediate/unfolded transitions; the majority of the changes in these parameters occurs in the first transition. These results suggest that the thermal unfolding reaction of des-Cys dihydrofolate reductase involves a stable intermediate whose properties resemble those of a molten globule.

A complete characterization of the native conformation of a protein requires not only a high resolution structure but also a thermodynamic analysis of its reversible transition to a suitable reference state, usually an unfolded form. The most common approaches employed to obtain these data involve studies of the chemical- or heat-induced unfolding reactions (Pace, 1986; Privalov & Potekhin, 1986). Chemical denaturants such as urea or guanidine hydrochloride can offer high reversibility and access to unfolded forms which retain little residual structure. These advantages are offset by complexities arising from an accurate assessment of the free energy of folding in the absence of denaturant. Several methods of extrapolation from the data obtained in unfolding transition regions have been proposed (Tanford, 1968; Pace, 1986), however, there is as yet no detailed analysis which accounts for the mechanism by which these reagents unfold proteins. An excellent discussion of this problem has been presented by Timasheff (1992).

Thermal unfolding, in contrast, rests on well-founded physical−chemical principles and leads naturally to several useful thermodynamic parameters including enthalpy, entropy, and heat capacity changes (Sturtevant, 1977; Freire & Biltonen, 1978; Privalov, 1979; Privalov & Gill, 1988; Sturtevant *et al.*, 1991). It also has the advantage of a straightforward extrapolation to standard conditions. Potential problems with thermal unfolding reactions, however, include incomplete reversibility, possibly reflecting chemical damage or aggregation, and the retention of residual structure in the unfolded form (e.g., Seshadri *et al.*, 1994). Although such residual structure could complicate comparisons with chemically-unfolded forms, an examination of the thermodynamic properties of chemically- and thermally-unfolded forms of apomyoglobin, cytochrome *c*, lysozyme, and ribonuclease A found that these two forms are closely similar when compared under the same solution conditions (Privalov, 1979; Privalov *et al.*, 1989; Privalov & Makhatadze, 1990). If these conclusions prove to be general, then the principal potential difficulty with the application of the thermal unfolding method is the problem of incomplete reversibility.

At high temperatures, proteins are subject to a variety of chemical reactions, many of which can affect the efficiency of the refolding reactions. These include the oxidation of sulfhydryls in cysteines, the deamidation of asparagines and glutamines, β-elimination of cystine cross-links, disulfide interchange, and the hydrolysis of the peptide backbone at Asp-X sequences (Feeney *et al.*, 1975; Ahern & Klibanov, 1988). The oxidation of cysteine residues by molecular oxygen, in particular, has long been recognized as the explanation for the thermal inactivation of many enzymes (e.g., Little & O'Brien, 1967). With the advent of molecular biology and the opportunity to replace specific amino acids with other naturally-occurring residues, it is now possible to circumvent this source of chemical damage. For example, the replacement of the single cysteine in bovine superoxide dismutase with alanine did not affect the activity at 21 °C but decreased by half the loss of activity for enzyme incubated at 70 °C (McRee *et al.*, 1990). Related to protein stability studies, the replacement of the two cysteines in T4 lysozyme with nonoxidizable side chains (Perry & Wetzel, 1987) greatly extends the range of pH and temperature over which this protein undergoes reversible unfolding transitions (Chen & Schellman, 1989; Hurley *et al.*, 1992).

† This study was supported by National Science Foundation Grant MCB 9317273 to C.R.M.

* Author to whom correspondence should be addressed.

‡ Present address: National Institute of Bioscience and Human Technology, and Joint Research Center for Atom Technology (JRCAT), National Institute for Advanced Interdisciplinary Research, 1-1 Higashi, Tsukuba Science City, Ibaraki 305, Japan.

® Abstract published in *Advance ACS Abstracts,* August 1, 1995.

[1] Abbreviations: DHFR, dihydrofolate reductase; K_2EDTA, dipotassium ethylenediaminetetraacetic acid; MTX, methotrexate; $NADP^+$, nicotinamide adenine dinucleotide phosphate, oxidized form; PAGE, polyacrylamide gel electrophoresis; DTNB, 5,5′-dithiobis(2-nitrobenzoic acid); UV, ultraviolet; CD, circular dichroism.

0006-2960/95/0434-10669$09.00/0

Dihydrofolate reductase (DHFR)[1] from *Escherichia coli* (5,6,7,8-tetrahydrofolate:$NADP^+$ oxidoreductase, EC 1.5.1.3) is a monomeric, α/β protein containing two nonessential cysteine residues among a total of 159 amino acids. The urea-induced unfolding reaction of DHFR is fully reversible and has been the source of a great deal of information about transient intermediates which appear during the refolding reaction (Touchette *et al.*, 1986; Frieden, 1990; Kuwajima *et al.*, 1991; Jennings *et al.*, 1993). Direct measurements of the thermodynamic parameters for the folding of wild-type DHFR, however, have been hampered by a lack of reversibility for the thermal transition (Uediara *et al.*, 1990a,b; Leontiev *et al.*, 1993). As a partial solution to this problem, Uedaira *et al.* (1990a) replaced Cys 152 with glutamic acid, a residue found at this position in DHFR from both *Salmonella typhimurium* and *Bacillus subtilis*. Although the thermal transition of C152E DHFR was more reversible than that of wild-type DHFR, less than 70% of the optical signal was recovered when the heated protein was refolded.

Expanding upon this observation, the double mutant in which Cys 85 was replaced with Ser and Cys 152 with Glu (C85S/C152E, des-Cys DHFR) was constructed. This double mutant is of particular interest because previous studies of the refolding reaction from high urea concentrations have shown that it displays simpler folding kinetics than wild-type protein (Iwakura *et al.*, 1993). Thus, it is a potentially useful reference system for testing the role of specific amino acids in folding by site-directed mutagenesis (Matthews, 1987; Goldenberg, 1988; Jennings *et al.*, 1991; Sancho & Fersht, 1992; Matthews, 1993). The thermal unfolding of this mutant was found to be fully reversible at concentrations below 15 μM and to involve a well-populated intermediate. This partially folded form may provide important clues to the folding reaction of DHFR.

MATERIALS AND METHODS

Chemicals, Bacterial Strains, and Mutagenesis. The methotrexate (MTX)−agarose affinity resin was purchased from Sigma, and the DEAE-Toyopearl 650M resin was obtained from Toso (Japan). Ultrapure urea was purchased from Scharz/Mann of ICN Biochemicals Inc. and used without further purification. Restriction enzymes and ligase were obtained from New England Biolabs or United States Biochemicals. All other chemicals were reagent grade.

E. coli strain AG1 (recA1, endA1, tyrA96, thi, hsdR17, supE44, and recA1) was used as a cloning host. The serine mutation at position 85 was introduced by oligonucleotide-directed mutagenesis (Kunkel *et al.*, 1987; Iwakura *et al.*, 1993). The glutamic acid replacement at position 152 was constructed by cassette mutagenesis using a plasmid, pTZ-DHFR, which contains 19 more unique restriction enzyme sites in or around the DHFR structural gene than the wild-type gene (Iwakura *et al.*, 1995). Mutations were confirmed by dideoxy sequencing of the entire gene.

Protein Purification and Activity Assay. Purification of wild-type and mutant DHFRs was achived using MTX affinity chromatography after several prepurification steps of a sonicated solution of the cell extract (Iwakura & Matthews, 1992). The wild-type and the mutant DHFRs were shown to be pure by the appearance of a single band on sodium dodecyl sulfate−PAGE (Laemmli, 1970) and on native PAGE (Davis, 1964).

The absence of cysteine in des-Cys DHFR was directly confirmed by the lack of an absorbance signal at 412 nm when the unfolded protein in 8 M urea was reacted with DTNB (data not shown). The two cysteines in wild-type DHFR were found to be readily modified by DTNB under the same conditions (K. E. Bowers and C. R. Matthews, unpublished results).

The concentrations of the mutant proteins were determined using absorbance spectroscopy and a molar extinction coefficient at 280 nm of 3.11×10^4 M^{-1} cm^{-1} previously determined for wild-type DHFR (Touchette *et al.*, 1986). This extinction coefficient was confirmed for the cysteine mutants examined in the present study using the Bradford method (Bradford, 1976). The enzymatic activity of des-Cys DHFR was determined as described by Hillcoat *et al.* (1967) to be 13.5 units mg^{-1} at 15 °C; the specific activity of wild-type DHFR in this assay was 13.8 units mg^{-1}.

Thermal Unfolding Experiments. Thermal unfolding experiments were carried out on a Cary 14DS UV−vis spectrophotometer modified by Aviv Associates. The sample was placed in a 10 mm cuvette with quartz stopper and heated in increments of 1 °C with a thermal electric cell holder. The sample was allowed to equilibrate for about 2 min before the absorbance at 292 nm was recorded. The samples were shown to be fully equilibrated by obtaining identical results with longer incubation times. After reaching the final temperature, the sample was cooled adiabatically by the same procedure and the absorbance recorded. The reversibility was monitored by the recovery of enzyme activity and by the comparison of the heating and cooling curves. When the thermal unfolding reaction was examined above 75 °C, it was necessary to cool the sample to 5 °C within 5 min to maintain the reversibility.

The far-UV circular dichroism signal at 222 nm was recorded in a 10 mm path length cell following a similar procedure on an Aviv 62DS circular dichroism spectrometer equipped with a Hewlett Packard 89100A temperature controller. The near-UV CD spectra were recorded using a 100 mm, water-jacketed cell.

The temperatures in both absorbance and CD experiments were measured with a thermocouple attached to the jacket of the cell holder. The thermocouple was calibrated against a standard provided by YSI, Inc. Control experiments with the thermocouple mounted inside the cuvette demonstrated the accuracy of the external reading.

The protein concentration was held constant in any individual experiment and ranged from 3 to 15 μM. The unfolding transition curve was found to be independent of the protein concentration when the protein concentration was held below 15 μM (data not shown). Above 15 μM, the thermal transition was not completely reversible. The buffer used in all thermal unfolding experiments contained 10 mM potassium phosphate and 0.2 mM K_2EDTA, pH 7.8.

Data Analysis. The optical data were converted to the apparent fraction of unfolded protein, F_{app}, by

$$F_{app} = (Y_o - Y_n)/(Y_u - Y_n) \quad (1)$$

where Y_o is the observed signal, and Y_u and Y_n are the optical signals for unfolded and native protein, respectively. Both the Y_u and Y_n were observed to depend linearly on the temperature; this linear dependence was assumed to hold in the transition region, and a linear fitting procedure was used

to obtain the temperature dependence of Y_n and Y_u. F_{app} is related to the apparent equilibrium constant, K_{app}, by:

$$K_{app} = F_{app}/(1 - F_{app}) \quad (2)$$

For the thermal unfolding experiments, both a two-state model and a three-state model were tested. For the two-state model, assuming ΔC_p is independent of temperature, it can be shown that

$$K_{app}(T) = \exp[-[\Delta S^\circ_m T_m/T - \Delta C_p(T - T_m)/T - \Delta S^\circ_m + \Delta C_p \ln(T_m/T)]]/R \quad (3)$$

where T_m is the melting temperature, ΔS°_m is the entropy difference at the melting temperature, and ΔC_p is the heat capacity difference. This equation is readily derived from the following thermodynamic relations:

$$K_{app}(T) = \exp[-(\Delta H^\circ(T) - T\Delta S^\circ(T))/RT] \quad (4)$$

$$\Delta H^\circ(T) = \Delta H^\circ_m + \Delta C_p(T - T_m) \quad (5)$$

$$\Delta S^\circ(T) = \Delta S^\circ_m + \Delta C_p \ln(T/T_m) \quad (6)$$

$$\Delta H^\circ_m = T_m \Delta S^\circ_m \quad (7)$$

where ΔH°_m is the enthalpy difference at the melting temperature and $\Delta H^\circ(T)$ and $\Delta S^\circ(T)$ are enthalpy and entropy differences as a function of the temperature.

The thermal unfolding data were also fit to a three-state model involving a native state, N, an intermediate state, I, and an unfolded state, U. At any temperature, the sum of the fractional population of the N state, F_N, the I state, F_I, and the U state, F_U, equals unity. It can be shown that F_{app} can be recast in terms of these populations as

$$F_{app} = F_U + ZF_I \quad (8)$$

where $Z = (Y_I - Y_N)/(Y_U - Y_N)$. This latter parameter describes the degree to which the I state resembles the U state. The fractional population of each state can be obtained from $F_N = Q_N/Q$, $F_I = Q_I/Q$, and $F_U = Q_U/Q$, respectively, where Q is the partition function for the three-state system. Choosing N as the reference state,

$$Q = Q_N + Q_I + Q_U \quad (9)$$

$$Q_N = 1 \quad (10)$$

$$Q_I = \exp(-\Delta G^\circ_{NI}/RT) \quad (11)$$

$$Q_U = \exp(-\Delta G^\circ_{NI}/RT)\exp(-\Delta G^\circ_{IU}/RT) \quad (12)$$

where ΔG°_{NI} and ΔG°_{IU} are the free energy differences between the N and I and the I and U states, respectively. ΔG°_{NI} and the ΔG°_{IU} can be reformulated in terms of the thermodynamic parameters introduced in eq 3:

$$\Delta G^\circ_{NI} = -\Delta S^\circ_{mNI} T_{mNI}/T + \Delta C_{pNI}(T - T_{mNI})/T + \Delta S^\circ_{mNI} - \Delta C_{pNI} \ln(T_{mNI}/T) \quad (13)$$

$$\Delta G^\circ_{IU} = -\Delta S^\circ_{mIU} T_{mIU}/T + \Delta C_{pIU}(T - T_{mIU})/T + \Delta S^\circ_{mIU} - \Delta C_{pIU} \ln(T_{mIU}/T) \quad (14)$$

where ΔS°_{mNI} and T_{mNI} relate to the temperature at the midpoint of the N to I transition, and ΔS°_{mIU} and T_{mIU} relate to the midpoint of the I to U transition. Finally, these expressions can be combined and substituted into eq 8 to yield an expression for F_{app} that contains seven independent parameters.

$$F_{app} = \frac{Z + \exp(-\Delta G^\circ_{NI}/RT)}{1 + \exp(-\Delta G^\circ_{NI}/RT) + \exp(-\Delta G^\circ_{IU}/RT)} \quad (15)$$

Data were fit to appropriate models using a nonlinear least-squares fitting program, NLIN (SAS Institute, Inc.). Native and unfolded base lines were determined either from a linear fit of the pre- (0−15 °C) and post-transition region data (75−95 °C for ABS and far-UV CD experiments, 50−70 °C for near-UV CD experiments) or from a fitting procedure similar to that of Santoro and Bolen (1988). The two procedures gave essentially identical results.

Global fitting of all absorbance, near-UV CD, and far-UV CD data was also performed using the same program. In this latter procedure, all thermodynamic parameters were constrained globally, while the optical properties of the intermediate (Z values) were allowed to vary for each spectroscopic method.

RESULTS

The thermal unfolding transitions of wild-type and des-Cys DHFR were monitored by both absorbance and circular dichroism spectroscopy. The UV absorbance at 292 nm (A_{292}) monitors the exposure of the five partially or fully buried tryptophan residues to aqueous solvent upon unfolding, i.e., the disruption of the tertiary structure. The CD signal in the near-UV region is sensitive to the packing of aromatic side chains in asymmetric environments and provides a complementary probe of tertiary structure. The far-UV CD signal at 222 nm contains contributions from the helices, strands, and turns and offers a measure of the disruption of secondary structure. Comparisons of the unfolding transitions obtained from these different probes provide a method of choosing the appropriate thermodynamic model.

The thermal unfolding transitions of the wild-type and des-Cys DHFRs, monitored by the changes in absorbance at 292 nm, are shown in Figure 1. The absorbance of the wild-type DHFR displayed little variation between 5 and 15 °C, consistent with a stable native conformation at low temperature (Figure 1A). Above 15 °C, A_{292} decreased in a sigmoidal fashion before approaching a linear decrease with temperature above 65 °C. When this sample was cooled, only a partial recovery of the signal was obtained (Figure 1A). Wild-type DHFR recovered 30% of the difference in absorbance between native and unfolded forms and 24% of the enzymatic activity when the temperature was lowered to 5 °C.

The thermal transition for the des-Cys DHFR also began near 15 °C and reached completion by 65 °C (Figure 1B). In striking contrast to the wild-type protein, the refolding transition for this double mutant was fully reversible. This reversibility was confirmed by the recovery of 100% of the enzymatic activity in the cooled sample. The thermal unfolding of five other cysteine-free mutants, C85A/C152E, C85G/C152E, C85A/C152S, C85S/C152S, and C85E/C152E

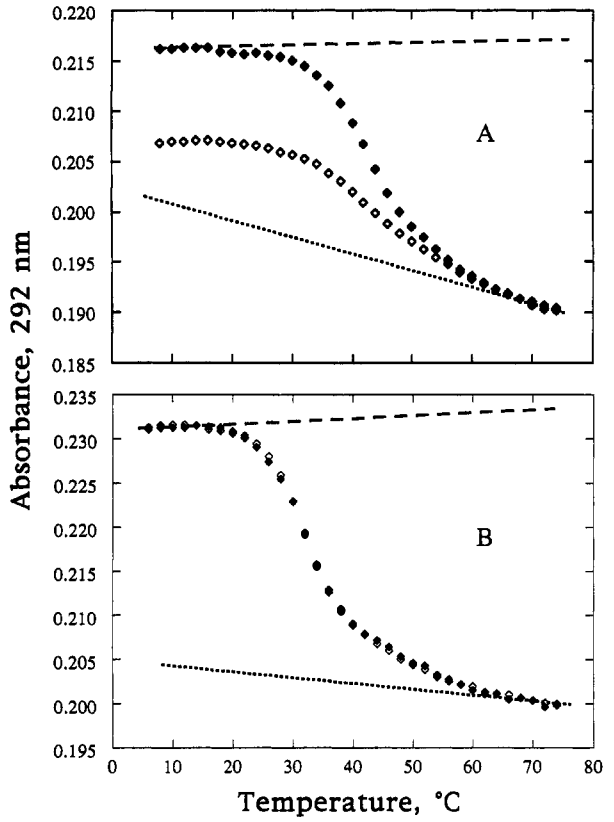

FIGURE 1: Thermal unfolding transitions for (A) wild-type DHFR and (B) C85S/C152E des-Cys DHFR, monitored by UV absorbance spectroscopy at 292 nm. Closed symbols correspond to the unfolding reaction, and the open symbols correspond to refolding. Native and unfolded base lines are drawn as dashed and dotted lines, respectively. The buffer contained 10 mM potassium phosphate and 0.2 mM K_2EDTA, pH 7.8. The sample concentrations for both experiments were 11 μM.

also displayed greater than 95% reversibility as judged by recovery of absorbance spectra, far-UV CD spectra, and enzyme activity (data not shown). Taken together, these results support the hypothesis that the chemical modification of one or both of the two cysteines in wild-type DHFR is responsible for the irreversibility of its thermal unfolding transition.

The thermal unfolding transition of des-Cys DHFR was also monitored by measuring the changes in ellipticity (θ) at both 222 and 292 nm. The results are shown in Figure 2. The shape of the far-UV CD transition (Figure 2A) is very similar to that for the absorbance change (Figure 1B), with a sigmoidal decrease in ellipticity beginning near 15 °C and approaching a constant, small linear increase above 65 °C. The transition monitored by the near-UV CD signal at 292 nm was quite different (Figure 2B). Although the lower signal/noise ratio at this wavelength led to greater scatter in the data, the decrease in θ_{292} began at about 20 °C and was complete at 45 °C. The CD signal near 287 nm, reflecting the behavior of one or more of the four tyrosine residues, also disappeared around 45 °C (data not shown). The 5-fold smaller magnitude of this signal prohibited quantitative measurements.

These three transition curves can be compared by converting the data to apparent fraction of unfolded protein, F_{app}, as described in Materials and Methods. None of these F_{app} curves are coincident (Figure 3), demonstrating that the thermal unfolding transition must involve at least one stable

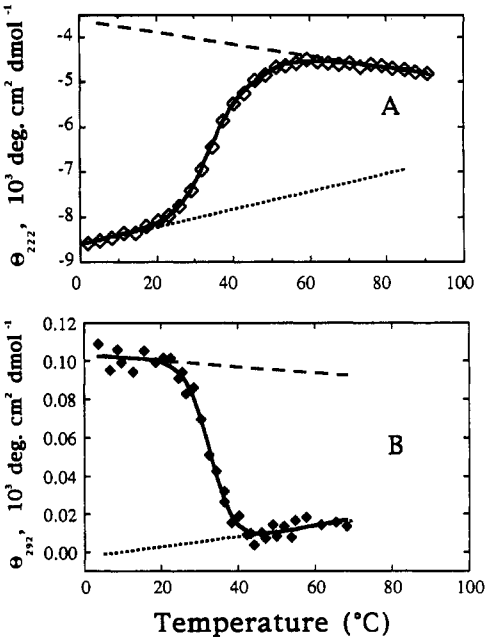

FIGURE 2: Thermal unfolding transitions for des-Cys DHFR, monitored by UV circular dichroism at (A) 222 nm and (B) 292 nm. The solid lines through the data points display the predicted values of a three-state analysis for the 222 nm data, and a two-state analysis for the 292 nm data. Native and unfolded base lines are shown as dashed and dotted lines, respectively. The buffer is described in the caption to Figure 1. The sample concentrations for both experiments were 3 μM.

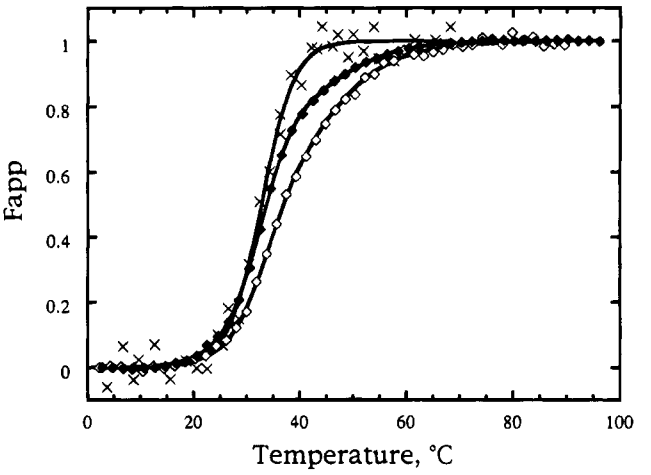

FIGURE 3: Apparent fraction of unfolded protein, calculated from the absorbance (♦), far-UV CD (◇), and near-UV CD (×) data in Figures 1 and 2 as the function of the temperature. Three-state fits of the absorbance at 292 nm and the ellipticity at 222 nm, and a two-state fit of the ellipticity at 292 nm, are shown as solid lines.

intermediate (Robson & Pain, 1976; Creighton & Pain, 1980; Ptitsyn *et al.*, 1990). Consistent with this observation, the F_{app} curves calculated from the UV absorbance changes at different wavelengths from 250 to 320 nm are also not coincident (data not shown). The inflections in both the absorbance and far-UV CD curves near 40 °C and the absence of further change in the near-UV CD curve above the same temperature suggest a three-state model with a highly populated intermediate near 40 °C: N ↔ I ↔ U.

The absorbance and far-UV CD data were fit to the above three-state model and the near-UV data to a two-state model; the thermodynamic parameters are listed in Table 1. Also listed in Table 1 are the results of a global fit which included

Table 1: Thermodynamic Parameters for the Three-State Folding Model for Des-Cys DHFR[a]

	ABS[b]	far-UV CD[c]	near-UV CD[d]	global fit[e]
T_{mNI} (°C)	33.1 ± 0.4	33.4 ± 0.7	32.9 ± 0.9	33.3 ± 0.6
ΔS_{mNI} (cal mol^{-1} K^{-1})	177 ± 5	167 ± 9	198 ± 3	177 ± 5
ΔH_{mNI} (kcal mol^{-1})	54 ± 3	51 ± 6	61 ± 9	54 ± 3
ΔC_{pNI} (cal mol^{-1} K^{-1})	1320 ± 140	1070 ± 320	869 ± 3150	1280 ± 240
T_{mIU} (°C)	45.8 ± 1.9	47.1 ± 3.7	N/A	46.2 ± 2.5
ΔS_{mIU} (cal mol^{-1} K^{-1})	87 ± 6	110 ± 30	N/A	94 ± 7
ΔH_{mIU} (kcal mol^{-1})	28 ± 2	35 ± 10	N/A	30 ± 3
ΔC_{pIU} (cal mol^{-1} K^{-1})	367 ± 250	0 ± 340	N/A	240 ± 260
Z[f]	0.72 ± 0.04	0.65 ± 0.08	N/A	0.76 ± 0.08 (ABS) 0.65 ± 0.15 (CD)

[a] Parameters and errors reported in the ABS and far-UV CD columns are statistical averages and standard deviations of 6 and 5 replicate experiments, respectively. Errors reported in near-UV CD and global fit columns are 95% confidence levels calculated by the fitting programs. [b] Absorbance at 292 nm. [c] Circular dichroism at 222 nm. [d] Circular dichroism at 292 nm. [e] Global fit of 6 ABS, 5 far-UV CD, and 1 near-UV CD data sets. Z values for the ABS and CD curves were allowed to vary independently and yield essentially identical values to those from individual fits of each data set. [f] Z value reflects the extent to which the intermediate resembles the unfolded state.

6 data sets obtained from absorbance, 5 from far-UV CD and 1 from near-UV CD spectroscopy.

The melting temperature, enthalpy, entropy, and the heat capacity for the first transition detected by absorbance and far-UV CD spectroscopy and the only transition detected by the near-UV CD spectroscopy are in good agreement. The global fit of all data yields a T_{mNI} of 33.3 ± 0.6 °C, a $\Delta H°_{mNI}$ of 54 ± 3 kcal mol^{-1}, a $\Delta S°_{mNI}$ of 177 ± 5 cal mol^{-1} K^{-1}, and a ΔC_{pNI} of 1280 ± 240 cal mol^{-1} K^{-1}. The factor which differentiates the absorbance and far-UV CD transition curves (Figure 3) is the optical property of the intermediate. From the global fit, the fractional change of signal in the intermediate, i.e., the Z value, for tryptophan absorbance is 0.76 ± 0.08 while that for the far-UV CD is 0.65 ± 0.15 (Table 1). Although the magnitude of the errors for these Z values is comparable to the difference between them, the consistent displacement of the absorbance curve to lower temperature than the far-UV CD curve (Figure 3) shows that the difference is real. These data indicate that the tryptophans in the intermediate are solvated to a greater extent than the secondary structure is disrupted.

The thermodynamic parameters determined for the I ↔ U transition from both absorbance and far-UV CD data are in good agreement, considering the uncertainties. On the basis of the global fit, T_{mIU} is 46.2 ± 2.5 °C, $\Delta H°_{mIU}$ is 30 ± 3 kcal mol^{-1}, $\Delta S°_{mIU}$ is 94 ± 7 cal mol^{-1} K^{-1}, and ΔC_{pIU} is 245 ± 260 cal mol^{-1} K^{-1}. The absence of an accompanying change in the near-UV CD signal demonstrates that the tryptophan residues, while not fully exposed to solvent, are no longer constrained in the asymmetric environments found in the native conformation. The maximum fraction of this intermediate can be calculated from these data and, at 39 °C, is 65% of the population.

The unfolding and refolding transitions of des-Cys DHFR were found to be independent of protein concentration in the range of 3−15 μM (data not shown). Although refolding is not completely reversible above 15 μM, the unfolding curves in this concentration range display no apparent protein concentration dependence (data not shown). Analysis of these irreversible unfolding curves yields identical thermodynamic parameters within experimental errors.

DISCUSSION

The replacement of two nonessential cysteine residues in *E. coli* DHFR with nonoxidizable side chains has produced a variant which is fully reversible to thermal unfolding. Unlike the two-state urea unfolding process exhibited by the same mutant, C85S/C152E (Iwakura *et al.*, 1993), a highly populated intermediate, appears near 39 °C for the thermal transition. Far-UV circular dichroism spectroscopy indicates that this species has significant secondary structure, approximately 35% of that for the native conformation. Absorbance and near-UV CD spectroscopy show that the five tryptophan residues become largely but not completely hydrated and are no longer constrained in the tightly packed asymmetric environment characteristic of the native conformation. The near-UV CD signal from the four tyrosine residues also disappears, indicating that specific tertiary interactions around these residues are also lost in the intermediate.

Comparison of the thermodynamic properties of this intermediate relative to native and unfolded forms can be done with greatest accuracy at 46 °C, the midpoint of the I to U transition. This choice minimizes the errors in calculating the parameters for the I ↔ U transition at any other temperature, errors which reflect the substantial uncertainty in ΔC_{pIU} (Table 1). Base on the global fitting results in Table 1 and equations provided in the Materials and Methods section, $\Delta H°_{NI}$ = 70 kcal mol^{-1} and $\Delta S°_{NI}$ = 230 cal mol^{-1} K^{-1} at 46 °C. Comparison with the values for the I ↔ U transition (Table 1) shows that enthalpy, entropy, and heat capacity differences between N and I are substantially larger than those between I and U. At 46 °C, the relative magnitudes of $\Delta H°$, $\Delta S°$, and ΔC_p for the N ↔ I transition are 70%, 71% and 84%, respectively, of those between N and U. The differences in $\Delta H°$ and $\Delta S°$ between the two transitions diminish at lower temperature, due to the relative magnitudes of the ΔC_p terms. Despite the large uncertainty in the value of ΔC_{pIU}, these thermodynamic parameters for the N ↔ I transition remain larger than those for the I ↔ U transition at 15 °C.

The structural properties of this thermal intermediate in DHFR are very similar to those expected for a molten globule (Kuwajima, 1989; Ptitsyn *et al.*, 1990). Studies on a variety of proteins, usually under mildly denaturing conditions, acidic pH, or elevated temperature, have shown these species are relatively compact, contain significant secondary structure, and lack specific, well-defined tertiary structure (Dolgikh *et al.*, 1981; Ohgushi & Wada, 1983; Kuroda *et al.*, 1992; Barrick & Baldwin, 1993).

The thermodynamic properties of the molten globule state are more diverse, suggesting that they may be dependent on the protein system. In apomyoglobin and apo-α-lactalbumin, the unfolding of their molten globule states by temperature was observed to not follow a first order transition (Griko & Privalov, 1994; Griko *et al.*, 1994). In other cases, cooperative thermal unfolding transitions have been observed between molten globule states and the unfolded states (Bychkova *et al.*, 1992; Gittis *et al.*, 1993; Hagihara *et al.*, 1994). The thermodynamic behavior of the des-Cys DHFR more closely resembles that for the latter group of proteins, demonstrating that the thermal intermediate is a well-defined thermodynamic state.

The argument that the multistate unfolding behavior observed for des-Cys DHFR can be attributed to a stable, molten globule-like intermediate is strengthened by examining two alternatives. (1) DHFR is known to have two structural domains: residues 38−88, which form the adenine-binding domain, and residues 1−37 and 89−159, which form a large, discontinuous domain (Bystroff & Kraut, 1991). The possibility of independent domain unfolding is unlikely, considering the near-UV CD data, which show an absence of signal from all three tryptophans and four tyrosines in the larger domain and the two tryptophans in the smaller domain. The larger domain has clearly lost native-like tertiary packing since all four tyrosines in des-Cys DHFR are located in the larger domain. If the smaller domain retains native-like tertiary packing in the intermediate, the two tryptophans in this domain, Trp 47 and Trp 74, which are part of a tightly packed hydrophobic core and have been previously shown to form an exciton pair (Kuwajima *et al.*, 1991), must not contribute significantly to the native near-UV CD spectra. Although it cannot be excluded on the basis of available data, this possibility seems unlikely. (2) The native conformation of DHFR consists of two major slowly-interconverting forms (Cayley *et al.*, 1981; Falzone *et al.*, 1991). The possibility that the observed intermediate represents the unfolding of the more stable native form can also be ruled out on the basis of an unfolded-like near-UV CD spectrum for the intermediate. However, these optical data cannot eliminate more complicated models; e.g., each of the two native forms unfolds through one or two stable intermediates.

The observation of a stable intermediate in a thermal unfolding reaction is relatively unusual. Calorimetric studies show that many proteins follow a two-state equilibrium mechanism, with equivalent van't Hoff and calorimetric enthalpies (Privalov, 1979; Privalov & Potekhin, 1986). The presence of the intermeidate in des-Cys DHFR is unlikely to result solely from the mutations because the transition curve for wild-type DHFR shows the same gradual decrease in absorbance at high temperature (45−65 °C) as does the des-Cys DHFR (Figure 1, panels A and B). As a result, these data for the wild-type protein are also better described by a three-state model (data not shown). Some as yet not understood aspect of the sequence and/or structure of DHFR apparently leads to a molten globule form whose melting temperature exceeds that of the native conformation. Although this might be expected for the appropriate combination of thermodynamic parameters for the N/I and I/U transitions, it is curious that it is rarely observed. A similar situation occurs for the guanidine hydrochloride-induced unfolding of α-lactalbumin where a molten globule form is highly populated at intermediate denaturant concentration (Kuwajima, 1977). Most proteins display two-state behavior in chemical denaturation experiments (Pace, 1986; Tanford, 1968). The reasons for the multistate unfolding behavior of α-lactalbumin are also not known.

The existence of a stable molten globule form for DHFR is of fundamental interest. However, this species would gain additional significance if it could be shown to play a role in the actual folding mechanism. Stopped-flow CD studies of the refolding of urea-induced DHFR have shown that approximately 40% of the ellipticity at 222 nm is regained within 5 ms by an early intermediate which has marginal stability (Kuwajima *et al.*, 1991). In terms of mean residue ellipticity, the signal observed for this transient folding intermediate, -5×10^3 deg cm^2 dmol^{-1}, is comparable to that observed for the stable thermal intermediate (Figure 2A).

Although the secondary structures of these two species are similar, stopped-flow fluorescence spectroscopy (Garvey *et al.*, 1989) and time-resolved stopped-flow fluorescence spectroscopy (Jones *et al.*, 1995) suggest that the packing around the tryptophan residues is different. The tryptophans are fully exposed to solvent in the transient intermediate, unlike the partial exclusion observed in the thermal intermediate (Figure 1B). This difference in structure between the stable thermal intermediate and the transient urea intermediate could, however, reflect the differences in the temperature and solvent conditions at which these measurements were made. The stopped-flow data were collected at 15 °C in the presence of 0.4 M urea while the thermal data were collected at 39 °C in the absence of urea. In support of this explanation, the thermal unfolding transition observed by absorbance spectroscopy in the presence of 0.5 M urea is well characterized by a two-state transition; the CD transition curve still indicates the presence of the intermediate (J. Luo and C. R. Matthews, unpublished results).

These results suggest that the thermal intermediate in des-Cys DHFR could correspond to the early transient intermediate observed in refolding from high urea concentrations. This stable partially-folded form may provide useful information on the structure and thermodynamics properties of a short-lived folding intermediate and, thereby, enhance the understanding of the early events in the folding of DHFR.

REFERENCES

Ahern, T. J., & Klibanov, A. M. (1988) *Methods Biochem. Anal. 33*, 91−125.
Barrick, D., & Baldwin, R. L. (1993) *Protein Sci. 2*, 869−876.
Bradford, M. M. (1976) *Anal. Biochem. 72*, 248−254.
Bychkova, V. E., Berni, R., Rossi, G. L., Kutyshenko, V. P., & Ptitsyn, O. B. (1992) *Biochemistry 31*, 7566−7571.
Bystroff, C., & Kraut, J. (1991) *Biochemistry 30*, 2227−2239.
Cayley, P. J., Dunn, S. M. J., & King, R. W. (1981) *Biochemistry 20*, 874−879.
Chen, B.-L., & Schellman, J. A. (1989) *Biochemistry 28*, 685−691.
Creighton, T. E., & Pain, R. H. (1980) *J. Mol. Biol. 137*, 431−436.
Davis, B. J. (1964) *Ann. N.Y. Acad. Sci. 121*, 404−421.
Dolgikh, D. A., Gilmanshin, R. I., Brazhnikov, E. V., Bychkova, V. E., Semisotnov, G. V., Venyaminov, S., & Ptitsyn, O. B. (1981) *FEBS Lett. 136*, 311−315.
Falzone, C. J., Wright, P. E., & Benkovic, S. J. (1991) *Biochemistry 30*, 2184−2191.
Feeney, R. E., Blankenhorn, G., & Dixon, H. B. F. (1975) *Adv. Protein Chem. 19*, 135−203.
Freire, E., & Biltonen, R. L. (1978) *Biopolymers 17*, 463−479.

Frieden, C. (1990) *Proc. Natl. Acad. Sci. U.S.A. 87*, 4413−4416.
Garvey, E. P., Swank, J., & Matthews, C. R. (1989) *Proteins 6*, 259−266.
Gittis, A. G., Stites, W. E., & Lattman, E. E. (1993) *J. Mol. Biol. 232*, 718−724.
Goldenberg, D. P. (1988) *Annu. Rev. Biophys. Biophys. Chem. 17*, 481−507.
Griko, Y. V., & Privalov, P. L. (1994) *J. Mol. Biol. 235*, 1318−1325.
Griko, Y. V., Freire, E., & Privalov, P. L. (1994) *Biochemistry 33*, 1889−1899.
Hagihara, Y., Tan, Y., & Goto, Y. (1994) *J. Mol. Biol. 237*, 336−348.
Hillcoat, B. L., Nixon, P. F., & Blakely, R. L. (1967) *Anal. Biochem. 21*, 178−189.
Hurley, J. H., Baase, W. A., & Matthews, B. W. (1992) *J. Mol. Biol. 224*, 1143−1150.
Iwakura, M., & Matthews, C. R. (1992) *Protein Eng. 5*, 791−796.
Iwakura, M., Jones, B. E., Falzone, C. J., & Matthews, C. R. (1993) *Biochemistry 32*, 13566−13574.
Iwakura, M., Jones, B. E., Luo, J., & Matthews, C. R. (1995) *J. Biochem. (Tokyo) 117*, 480−488.
Jennings, P. A., Saalau-Bethell, S. M., Finn, B. E., Chen, X., & Matthews, C. R. (1991) *Methods Enzymol. 202*, 113−126.
Jennings, P. A., Finn, B. E., Jones, B. E., & Matthews, C. R. (1993) *Biochemistry 32*, 3783−3789.
Jones, B. E., Beechem, J. M., & Matthews, C. R. (1995) *Biochemistry 34*, 1867−1877.
Kunkel, T. A., Roberts, J. D., & Zakour, R. A. (1987) *Methods Enzymol. 154*, 367−383.
Kuroda, Y., Kidokoro, S., & Wada, A. (1992) *J. Mol. Biol. 223*, 1139−1153.
Kuwajima, K. (1977) *J. Mol. Biol. 114*, 241−258.
Kuwajima, K. (1989) *Proteins 6*, 87−103.
Kuwajima, K., Garvey, E. P., Finn, B. E., Matthews, C. R., & Sugai, S. (1991) *Biochemistry 30*, 7693−7703.
Laemmli, U. K. (1970) *Nature 227*, 680−685.
Leontiev, V. V., Uversky, N. V., & Gudkov, T. A. (1993) *Protein Eng. 16*, 81−84.
Little, C., & O'Brien, P. J. (1967) *Arch. Biochem. Biophys. 122*, 406−410.
Matthews, B. W. (1993) *Annu. Rev. Biochem. 62*, 139−160.
Matthews, C. R. (1987) *Methods Enzymol. 154*, 498−511.
McRee, D. E., Redford, S. M., Getzoff, E. D., Lepock, J. R., Hallewell, R. A., & Tainer, J. A. (1990) *J. Biol. Chem. 265*, 14234−14241.
Ohgushi, M., & Wada, A. (1983) *FEBS Lett. 164*, 21−24.
Pace, C. N. (1986) *Methods Enzymol. 131*, 266−280.
Perry, L. J., & Wetzel, R. (1987) *Protein Eng. 1*, 101−105.
Privalov, P. L. (1979) *Adv. Protein Chem. 33*, 167−241.
Privalov, P. L., & Potekhin, S. A. (1986) *Methods Enzymol. 131*, 4−51.
Privalov, P. L., & Gill, S. J. (1988) *Adv. Protein Chem. 39*, 191−234.
Privalov, P. L., & Makhatadze, G. I. (1990) *J. Mol. Biol. 213*, 385−391.
Privalov, P. L., Venyaminov, S., Yu, S., Tiktopulo, E. I., Griko, Y. V., Makhatadze, G. I., & Khechinashvili, N. N. (1989) *J. Mol. Biol. 205*, 737−750.
Ptitsyn, O. B., Pain, R. H., Semisotnov, G. V., Zerovnik, E., & Razgulyaev, O. I. (1990) *FEBS Lett. 262*, 20−24.
Robson, B., & Pain, R. H. (1976) *Biochem. J. 155*, 325−330.
Sancho, J., & Fersht, A. R. (1992) *J. Mol. Biol. 224*, 741−747.
Santoro, N. M., & Bolen, D. W. (1988) *Biochemistry 27*, 8063−8068.
Seshadri, S., Oberg, K. A., & Fink, A. L. (1994) *Biochemistry 33*, 1351−1355.
Sturtevant, J. M. (1977) *Proc. Natl. Acad. Sci. U.S.A. 74*, 2236−2240.
Sturtevant, J. M., Holtzer, M. E., & Holtzer, A. (1991) *Biopolymers 31*, 489−495.
Tanford, C. (1968) *Adv. Protein Chem. 23*, 121−282.
Timasheff, S. N. (1992) *Biochemistry 31*, 9857−9864.
Touchette, N. A., Perry, K. M., & Matthews, C. R. (1986) *Biochemistry 25*, 5445−5452.
Uediara, H., Kidokoro, S., Iwakura, M., Honda, S., & Ohashi, S. (1990a) *Ann. N.Y. Acad. Sci. 613*, 352−357.
Uediara, H., Kidokoro, S., Iwakura, M., Honda, S., & Ohashi, S. (1990b) *Thermochimim. Acta 163*, 123−128.

BI950916W